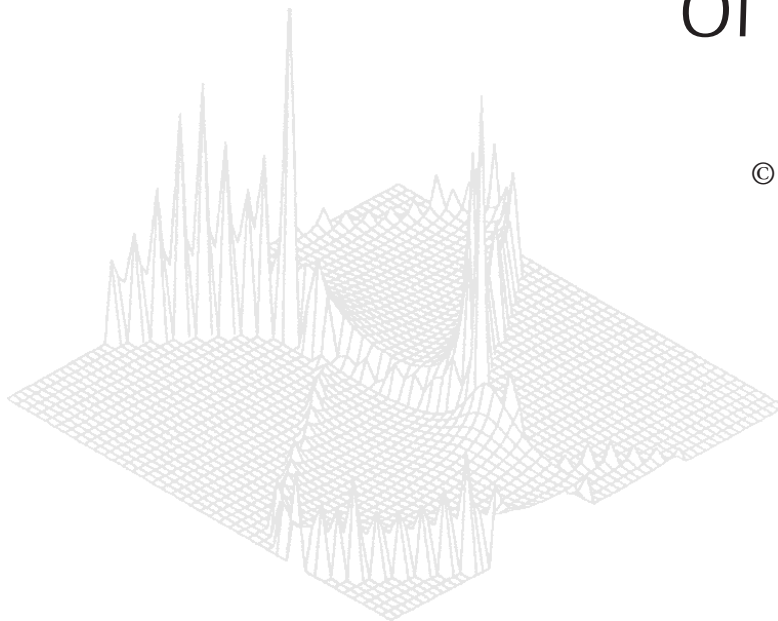

C S I R O P U B L I S H I N G

Australian Journal of Physics

Volume 50, 1997
© CSIRO Australia 1997



A journal for the publication of
original research in all branches of physics

www.publish.csiro.au/journals/ajp

All enquiries and manuscripts should be directed to

Australian Journal of Physics

CSIRO PUBLISHING

PO Box 1139 (150 Oxford St)

Collingwood

Vic. 3066

Australia

Telephone: 61 3 9662 7626

Facsimile: 61 3 9662 7611

Email: peter.robertson@publish.csiro.au



Published by **CSIRO PUBLISHING**
for CSIRO Australia and
the Australian Academy of Science



Potential Energy Surfaces for Unsaturated Hydrocarbons from Crossed Molecular Beams*

K. P. Stevenson, J. D. Close,^A P. L. Muiño^B and R. O. Watts

School of Chemistry, University of Melbourne,
Parkville, Vic. 3052, Australia, and
Department of Chemistry, University of Washington,
Seattle, WA 98195-1700, USA.

^A Present address: Max Planck Institut für Strömungsforschung,
Gottingen, Germany.

^B Present address: Department of Chemistry, Kansas State University,
Manhattan, KS 66506, USA.

Abstract

The total differential scattering cross sections for several important unsaturated hydrocarbon molecules with common atmospheric gases were measured in a crossed molecular beam apparatus. The experiments show quantum interferences which relate to potential energy surface parameters, such as the well depth and radial minimum. The damping of the quantum features, over contributions from experimental resolutions, provides information on the angular and radial anisotropies present in the potential energy surfaces. We have investigated two areas: (1) the role of the probe partner in determining the interaction strength for a given hydrocarbon target, and (2) the effect of increasing the overall length of the hydrocarbon molecule for a fixed probe. By comparing results for a class of scattering systems, we can identify chemical and physical trends that determine the van der Waals potential energy surfaces of larger molecules. We expect these results to aid in the prediction and interpretation of complementary experimental measurements on the high resolution infrared spectroscopy of weakly bound complexes.

1. Introduction

High-resolution infrared (IR) spectroscopy and crossed molecular beam scattering methods provide complementary information on van der Waals interactions. When combined in a quantum mechanical analysis, improvements to model potential energy surfaces over the full angular and radial range are usually achieved. High-resolution near and far IR spectroscopy of weakly bound complexes provides direct information concerning the equilibrium structure, and the intra- and intermolecular vibrational dynamics probes the potential in the region of the minimum. IR spectroscopic studies are usually limited to systems with relatively large interaction strengths and where one of the monomeric constituents has a significant infrared absorption strength. These spectra can be complicated by characteristic large amplitude, anharmonic motions and by rotational–vibrational tunneling in the complex. Both these conditions lead to difficulties in assigning observed transition frequencies with ‘good’ quantum numbers. In many cases the interpretation and assignment of IR spectroscopic transitions is aided by

* Dedicated to Professor Robert W. Crompton on the occasion of his seventieth birthday.

knowledge of the potential energy surface at orientations other than the global minimum (Weida *et al.* 1994; Moszynski *et al.* 1995).

Crossed molecular beam scattering methods are able to provide information on the full potential energy surface, depending on the relative collision energy and the angular range of the scattering distribution. Integral scattering cross sections measured as a function of collision energy provide information on the attractive, long-range part of the potential energy surface. Differential scattering cross sections probe both the long-range part of the potential, at small scattering angles, and the short range repulsive part of the potential, at large scattering angles. State-to-state integral and differential cross sections measured at thermal collision energies probe rotational energy transfer, which is most sensitive to anisotropy in the repulsive part of the potential energy surface.

The differential scattering cross sections of hydrocarbon molecules have been investigated previously. Danielson and coworkers measured the total differential scattering of He from C₂H₂, C₂H₄, C₂H₆ and CHF₃ (Danielson *et al.* 1987, 1988). Este *et al.* (1983) have investigated atomic H scattering from C₂H₆, C₃H₈, and C₂H₂. Rare gas-CH₄ scattering has been studied in the past by Buck (Buck *et al.* 1983, 1985*a*, 1985*b*) and more recently by Nesbitt (Nesbitt *et al.* 1993; Schiffman *et al.* 1996).

In earlier work we presented both spectroscopic and scattering measurements in which acetylene, C₂H₂ was the molecule of primary interest (Bryant *et al.* 1988; Beck *et al.* 1993; Yang and Watts 1994*a*, 1994*b*; Buck *et al.* 1993). Most recently, we analysed scattering and spectroscopic data for the system Ar-C₂H₂ using several potential energy surfaces taken from the literature (Yang and Watts 1994*b*). This analysis suggested that long cylindrical molecules might be expected to have large, strongly inelastic ($\Delta j \geq 6$), scattering cross sections at small centre-of-mass scattering angles, corresponding to large impact parameter collisions. Physically, such large transfer cross sections correspond to impacts at the end of a long lever arm, when rotational energy transfer is especially favoured and translational deflection is minimal. Accordingly, we set out to probe the possibility of detecting such unusually large cross sections and at the same time to lay the groundwork for a better understanding of interactions between unsaturated hydrocarbons and simple atomic and diatomic species. The present paper is an initial report on this study.

The unsaturated hydrocarbon molecules considered in this paper are acetylene, C₂H₂, ethylene, C₂H₄, allene, C₃H₄, and diacetylene, C₄H₂. All these molecules have linear arrangements of double and triple C-C bonds, and their potential energy surfaces with atomic and simple diatomic species are expected to be essentially cylindrical with several equivalent minimum energy configurations. As probe species we have used the inert gases He, Ne and Ar, and the diatomic molecules H₂, N₂, CO and NO. Large amplitude bending vibrations and rotational-vibrational tunneling will be important in van der Waals dimers formed from these collision partners and we plan future spectroscopic studies to probe such motions. The availability of thermal energy scattering information will help in understanding the spectroscopy of these systems and lead to improved potential energy surfaces that may be used in other calculations. Here, we summarise our measured cross sections and report the results of a preliminary analysis designed to identify important anisotropies in the potential energy surfaces.

2. Experimental

The total differential scattering cross sections were measured using a crossed molecular beam apparatus that has been described previously (Boughton *et al.* 1986). Primary and secondary beams were produced by supersonic expansion of probe and target gases through 50 μm diameter pinhole nozzles in separate differentially pumped source chambers. Angular collimation using two conical brass skimmers of 400 and 800 μm on the primary beam, and a 800 μm skimmer on the secondary beam, allowed the beams to intersect at approximately 90° on the rotational axis of a differentially pumped scattering chamber. The in-plane scattered flux was collected using a doped-Si bolometer operating near 1.8 K. Modulation of the secondary beam near 37 Hz provided the reference signal for phase sensitive, lock-in detection. Integration times for each data point varied between 3 and 8 minutes depending on the scattering angle.

Because the secondary beam modulation affects the background gas level in the scattering chamber, the signal was also recorded with the primary beam flagged at the same angle and integration conditions. To correct for changes in detector sensitivity and beam intensities, the signal at a chosen reference angle was remeasured every fourth data point and the data were renormalised. Linear interpolation was used to correct data points falling between the reference measurements. During the usual ten hours duration of a typical experimental session, the absolute variation in the reference signal was generally less than 10%. We estimate that the measured total differential scattering cross sections are accurate to $\pm 5\%$.

Most gases used in the experiments were commercially available with at least 99% purity; the allene was 97% pure. Diacetylene was synthesised from 1,4-dichloro-2-butyne and NaOH using a procedure described by Armitage *et al.* (1951). FTIR and mass spectroscopic analysis showed the purity of the diacetylene to be approximately 90%. Source stagnation pressures, chosen to optimise scattering signals and minimise clustering, were typically around 50 kPa for the hydrocarbon target molecules and 750 kPa for the probe gases. In all cases the hydrocarbons were admitted to the system through the secondary nozzle which means that for the heavier probe gases the detector was sometimes monitoring scattered fluxes from both beams. Typical working pressures in the primary, secondary and main differentially pumped chambers were about 10^{-4} , 10^{-4} , and 10^{-7} Torr respectively.

The velocity distributions and relative collision energy for each set of collision partners were determined by a time-of-flight analysis of each molecular beam under the experimental conditions used during the scattering measurements. The velocity resolutions of the atomic, diatomic, and molecular beams considered in this study are generally between 5–10%. The velocity distribution widths provide a rough estimate of the internal energy distribution, by assuming the translational, rotational, and vibrational degrees of freedom are in equilibrium. The diatomic probe molecules with relatively large rotational constants are cold, both with respect to translation and the internal degrees of freedom. The intramolecular modes of the hydrocarbons, which have much smaller rotational constants, are less relaxed. The rotational temperatures of acetylene, ethylene, allene and diacetylene were estimated to be 26, 32, 47 and 64 K respectively.

3. Potentials and Analysis

The measured cross sections show two types of quantum interference, rapid oscillations associated with the more repulsive part of the potential and rainbow maxima arising from deflections originating in the region of the potential minimum. A simple analysis based on spherical potentials shows that the angular spacing of these interferences can be used to give preliminary estimates of the position of the potential minimum R_m , and the well depth ϵ (Bernstein 1979*a*). In the case of the fast oscillations, the approximate value of R_m is given in terms of the angular spacing between diffraction maxima $\Delta\theta$ by

$$R_m = \frac{\lambda}{2\Delta\theta} = \frac{h}{2\mu g \Delta\theta}, \quad (1)$$

where λ is the de Broglie wavelength, h is Planck's constant, μ the reduced mass and g the relative speed of the collision partners. In the case of rainbow maxima θ_R , the potential well depth is given approximately by

$$\epsilon = \frac{\theta_R E_{\text{coll}}}{2} = \frac{\theta_R \mu g^2}{4}. \quad (2)$$

Formally, these formulae are applicable to spherical interactions described by a specific functional form but they serve to give empirical guidance when making a more substantial analysis. In the case of the present systems, both the rapid oscillations and the rainbow maxima are damped by anisotropies in the potential surfaces, making applications of the above formulae no more than qualitative.

For a more comprehensive analysis of the experimental measurements it is necessary to use models of the potential energy surface which allow for the anisotropy in the interactions. Several approaches can be used, including a sum of atom/atom terms, expansion of the full potential in spherical harmonics, and the use of functional forms fitted to *ab initio* calculations. In the present work we use a variation of a method described by Pack (1978), used with some success in our earlier analysis of the Ar-C₂H₂ scattering measurement (Yang and Watts 1994*a*, 1994*b*). The basic functional form used is that developed by Barker (Barker and Pompe 1968; Barker and Bobetic 1970),

$$V(R^*) = \epsilon \left[\exp[-\alpha(R^* - 1)]Q(R^*) - \sum_{n=6}^8 \frac{C_n^*}{(R^*)^n + 0.01} \right], \quad (3)$$

where $R^* = R/R_m$ and $Q(R^*)$ is a polynomial. The dispersion coefficients are chosen to be either the best available in the literature or estimated using combining rules (Amos and Yoffee 1976; Buckingham *et al.* 1988; Pack 1976). In order to introduce angular dependence to the potential, the parameters ϵ and R_m are expanded in spherical harmonics (Pack 1978) of the appropriate symmetry for the hydrocarbon under consideration. Parameters to be fitted to the experimental measurements are then the coefficients in these expansions. Typically, up to three terms are needed in both series and we made calculations using longer expansions to ensure that reasonable convergence was obtained.

We made a preliminary analysis of every set of data using single channel quantum calculations and a spherical potential, to determine starting values of ϵ and R_m . Once this was complete, we fitted anisotropic potentials to the scattering data using the infinite order sudden (IOS) approximation (Bernstein 1979*b*; Parker and Pack 1978). Typically, at least 32 different orientations were used in the angular averaging. In addition, the calculated cross sections were averaged over the angular and energy resolutions of the primary and secondary beams, and the detector, using methods described in earlier publications (Yang and Watts 1994*a*, 1994*b*; Boughton *et al.* 1986).

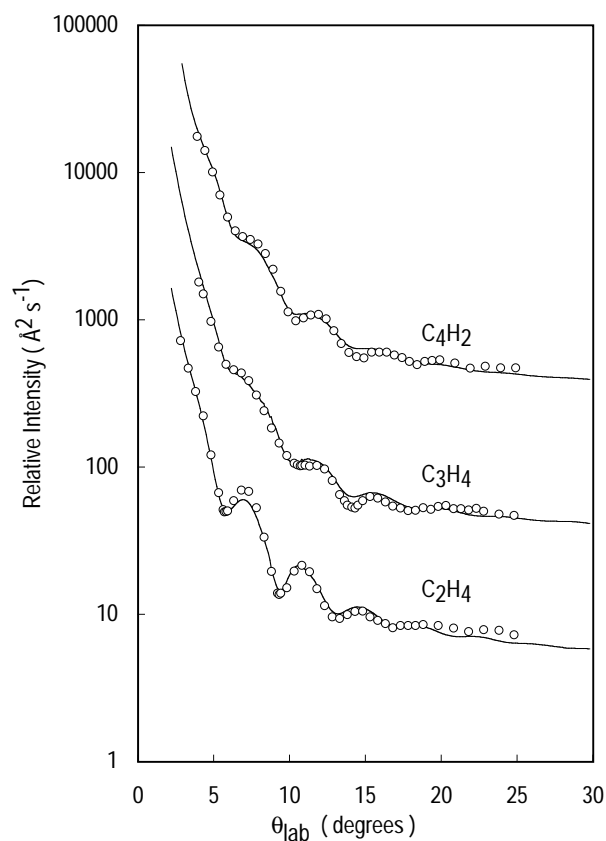


Fig. 1. Total differential cross sections of He with C_2H_4 , C_3H_4 and C_4H_2 at relative collision energies of 817, 824 and 826 K respectively. The curves are for a fitted anisotropic Barker potential using the IOS approximation.

4. Results

Fig. 1 compares total differential scattering cross sections for C_2H_4 , C_3H_4 and C_4H_2 with helium. In these cases the fast oscillations are clearly resolved. The data show that the oscillations become progressively more damped as the anisotropy (length) of the target molecule increases. Fig. 2 makes a corresponding comparison for scattering in which H_2 is the probe. Once again, only rapid

oscillations are detected and the damping increases with anisotropy. Comparing results for the same the target molecule but He or H₂ as the probe, we see two features of interest. First, the number of oscillations for H₂ as the probe is greater than when He is the scattering partner and secondly the damping is greater for H₂. The first of these results is a reflection of the fact that interactions between H₂ and the hydrocarbons are stronger than those in which He is the probe. It is well known that as the potential well depth increases, the number of resolvable diffraction oscillations also increases (Bernstein 1979*a*; Fluendy and Lawley 1973). The increased damping is a consequence of the greater anisotropy of the H₂ interaction compared with that for helium.

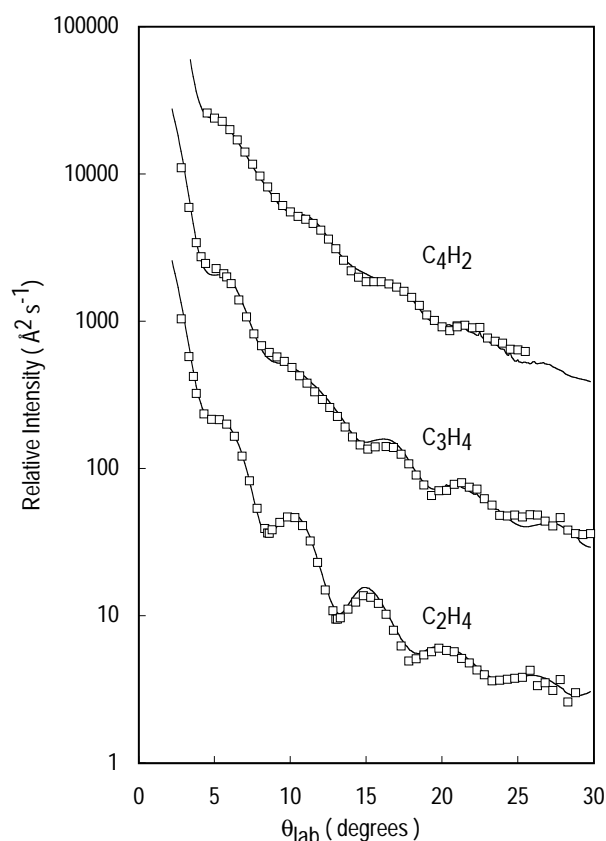


Fig. 2. Total differential cross sections of H₂ with C₂H₄, C₃H₄ and C₄H₂ at relative collision energies of 874, 880 and 880 K respectively. The curves are for a fitted anisotropic Barker potential using the IOS approximation.

The two figures also include best fit potential energy surfaces based on the anisotropic Barker model as described in the previous section. We considered several other functional forms before settling on this description, and found this one to be the most satisfactory. As described earlier, the parameter estimation was based on an IOS analysis of the data using methods described in earlier publications (Yang and Watts 1994*a*; Boughton *et al.* 1986). It should also be

noted that in these calculations the anisotropy of H_2 has been neglected by assuming that H_2 is a structureless (spherical) scattering partner. Table 1 reports values of the well depth and position of the minimum for the fitted potentials, both along the hydrocarbon symmetry axis and perpendicular to it, ϵ_{\perp} , ϵ_{\parallel} , $R_{m,\perp}$ and $R_{m,\parallel}$ respectively. Also given in the table are the corresponding values for C_2H_2 reported by Yang and Watts (Yang and Watts 1994a; Buck *et al.* 1993). The potential parameters show in a more quantitative way the features deduced on the basis of the diffraction oscillations.

Table 1. Summary of interaction parameters for He and H_2 with C_2H_2 , C_2H_4 , C_3H_4 and C_4H_2

System	$R_{m,\perp}$ (Å)	$R_{m,\parallel}$ (Å)	ϵ_{\perp} (K)	ϵ_{\parallel} (K)
He- $\text{C}_2\text{H}_2^{\text{A}}$	3.73	4.42	31	22
He- C_2H_4	3.68	4.59	39.5	17
He- C_3H_4	3.44	5.01	42.5	20
He- C_4H_2	3.41	6.18	49	13
H_2 - $\text{C}_2\text{H}_2^{\text{B}}$	3.38	4.11	126	73
H_2 - $\text{C}_2\text{H}_2^{\text{C}}$	3.67	4.40	85	85
H_2 - C_2H_4	3.66	4.45	92	92
H_2 - C_3H_4	3.44	5.04	130	130
H_2 - C_4H_2	3.44	5.94	146	146

^A Values from Buck *et al.* (1993).

^B Values from Yang and Watts (1994a).

^C Present results obtained from refitting data from Yang and Watts (1994a) with a corrected H_2 velocity distribution.

What is especially interesting is the difference between anisotropies in the well depth. The table shows that the strengths of all the He interactions vary considerably from the parallel to perpendicular configuration, with the latter configuration being significantly more stable. Surprisingly, the H_2 interactions remain of essentially the same depth at all orientations. Including anisotropy in the well depth for the H_2 interactions proved to be fairly insensitive to the overall quality of the fit. Calculations for the H_2 systems with ϵ_{\perp} 10–15% larger than ϵ_{\parallel} showed no improvement. Therefore, it was difficult to justify including additional parameters to characterise anisotropy in the well depth for these systems.

In the case of the He interactions, good quality fits were not possible without including some anisotropy in the well depth, but the overall absolute interaction strengths of the He systems compared to the H_2 systems are generally much smaller. The differences between the He and H_2 results could reflect different sensitivities to shapes in the corresponding potential energy surfaces. The H_2 potentials are more repulsive at short range with deeper, narrower potential wells, while the He potentials are less repulsive at short range with more shallow, broader potential wells. This result, while surprising, is consistent with previous findings where it has been established that diffraction oscillations are more sensitive to the radial minimum position anisotropy and less sensitive to the well depth and its anisotropy (Scoles 1988).

The present results for H_2 - C_2H_4 , H_2 - C_3H_4 , H_2 - C_4H_2 seem to disagree with the earlier H_2 - C_2H_2 results of Yang and Watts (1994a), which have much smaller radial minimum positions in the parallel and perpendicular orientations than any

of the other systems listed. Further analysis of the Yang and Watts $\text{H}_2\text{-C}_2\text{H}_2$ results, but using the velocity distribution for H_2 measured in this study, gave values in better agreement with the present findings. Parameters for both fits are given in Table 1.

Fig. 3 shows contour plots for the systems $\text{He-C}_4\text{H}_2$ and $\text{H}_2\text{-C}_4\text{H}_2$ where the difference in well depth anisotropies can be clearly distinguished. This analysis suggests that van der Waals dimers formed between the unsaturated hydrocarbons and H_2 are likely to be subject to very large amplitude internal librations; possibly even free internal rotation of monomer subunits in the complex. Spectroscopic studies of the dimers would be of considerable value in evaluating this prediction.

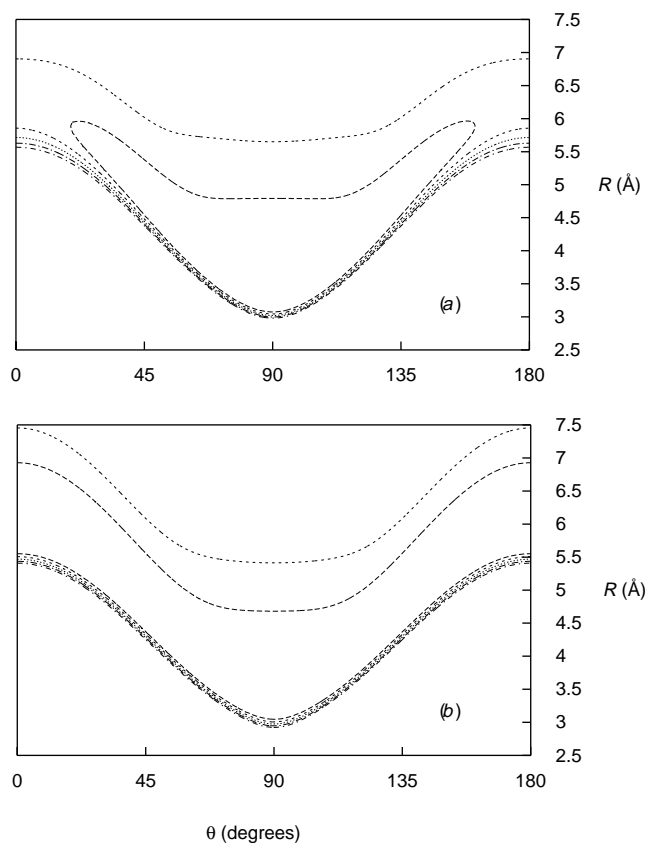


Fig. 3. Contour plot of the best fit anisotropic Barker potential for (a) $\text{He-C}_4\text{H}_2$ and (b) $\text{H}_2\text{-C}_4\text{H}_2$. For the He interaction, contours lines are 0, -10, -20, -30 and -40 K from the innermost contour. For the H_2 interaction, contours lines are 0, -30, -60, -90 and -120 K from the innermost contour.

Anisotropies in the positions of the potential minimum are in accordance with known molecular geometries and, for example, $R_{m,\parallel}$ increases with the length of the hydrocarbon in strict proportion to the number of chemical bonds along the symmetry axis. The anisotropies in the series $\text{C}_4\text{H}_2 > \text{C}_3\text{H}_4 > \text{C}_2\text{H}_4 > \text{C}_2\text{H}_2$ are consistent with the earlier study by Danielson *et al.* in which the anisotropies for C_2

containing hydrocarbons were observed to follow the sequence $C_2H_6 > C_2H_4 > C_2H_2$ (Danielson *et al.* 1988).

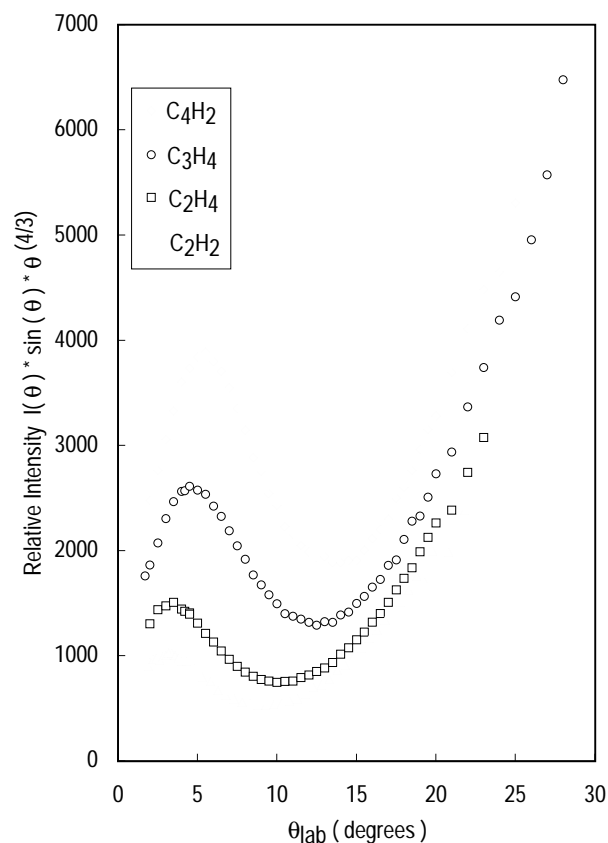


Fig. 4. Total differential cross sections for Ne with C_2H_2 , C_2H_4 , C_3H_4 and C_4H_2 at relative collision energies of 911, 928, 978 and 986 K respectively.

The total differential scattering cross sections for which Ne is the probe species are shown in Fig. 4. The scattering intensities shown have been weighted by an angular function to better show the scattering features. It is clear that the dominant oscillation arises from the rainbow effect. As the size of the hydrocarbon target molecule increases, the position of the rainbow maximum moves to larger angles and its amplitude increases. These two features are a consequence of the increasing interaction strength. A careful examination of the Ne- C_2H_2 cross section shows the presence of some oscillatory structure superimposed on the rainbow at small angles. In order to assess the possibility that these features arise from rapid oscillations we made careful measurements in which the angular resolution was improved significantly by increasing the distance between scattering centre and detector by a factor of about four. The results are shown in Fig. 5. It is clear from this figure that the Ne data show both rapid oscillations and a rainbow, allowing both the position of the potential minimum and the well depth

to be estimated. Fig. 5 also shows that the rapid oscillations become damped as the size of the hydrocarbon increases, due to the larger anisotropies of the longer molecules.

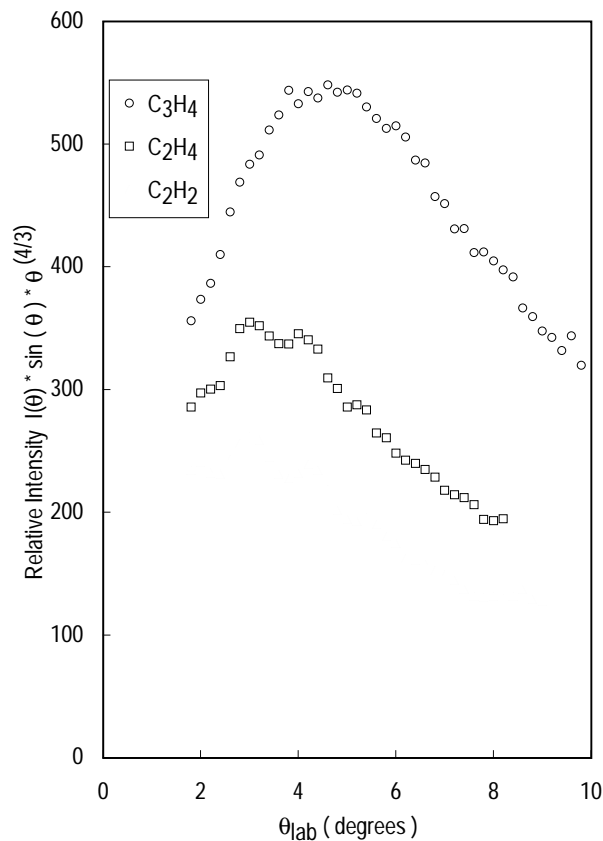


Fig. 5. Total differential cross sections for Ne with C_2H_2 , C_2H_4 and C_3H_4 at high angular resolution.

A spherical estimate of the position of the radial minimum for these systems can be obtained using equation (1). The average angular spacings in the centre-of-mass frame for Ne with C_2H_2 , C_2H_4 and C_3H_4 are 2.4° , 2.3° and 2.1° respectively, yielding R_m values of 3.63 \AA for acetylene, 3.69 \AA for ethylene, and 3.73 \AA for allene. While these results are qualitative at best, the correct trend of an increasing radial minimum position with increasing molecular size is indicated. A more complete IOS analysis of the Ne scattering results will indicate the anisotropies in these systems.

All the other scattering cross sections showed only rainbow maxima. As an example, Fig. 6 presents the results for the scattering of N_2 , CO and NO from C_2H_4 . Once again, the scattering intensities have been weighted by an angular function to better show the scattering features. The rainbow angles increase in the order $N_2 < CO < NO$, a sequence which corresponds to the interaction strengths. The same sequence is observed for the other systems and Table 2 summarises the

relevant information. This table also gathers together the isotropic well depths estimated using equation (2). Detailed analysis of the data, including estimates of anisotropies, will be reported in a subsequent publication.

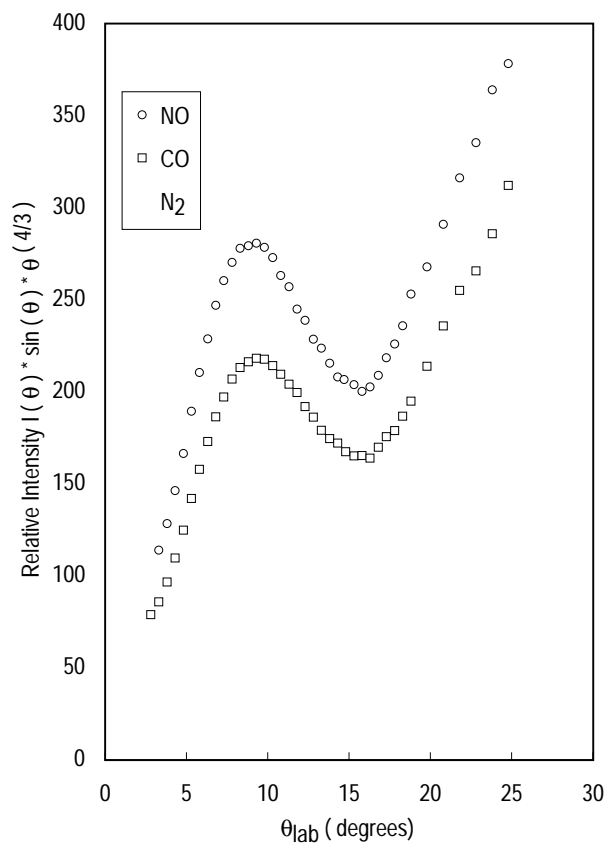


Fig. 6. Total differential cross sections for N_2 , CO and NO with C_2H_4 at relative collision energies of 1090, 1092 and 1106 K respectively.

Table 2. Spherical well depths for atomic and diatomic interactions with various unsaturated hydrocarbons, estimated using equation (2)

Probe	C_2H_2		C_2H_4		C_3H_4		C_4H_2	
	θ_R	ϵ (K)						
Ne	5.7	45	6.1	49	7.2	61	7.9	68
N_2	18.6 ^A	173	16.6	158	19.8	204		
CO	20.2	188	18.6	177	20.9	216		
NO	23.0	217	20.2	195	23.2	244		
Ar	19.5 ^B	162	19.9	170	24.0	223	25.8	245

^A Values for $\text{N}_2\text{-C}_2\text{H}_2$ reproduced from Yang and Watts (1994a).

^B Values for $\text{Ar-C}_2\text{H}_2$ reproduced from Yang and Watts (1994a).

5. Summary and Conclusions

We have given an overview of a comprehensive series of scattering experiments designed to probe the interactions of unsaturated hydrocarbons with simple atomic and diatomic species. Two types of diffraction oscillation have been identified, rapid oscillations which probe the effective sizes of the molecules and rainbow oscillations which are sensitive to the well depth. Rapid oscillations are found for the probe species He and H₂; rainbow maxima for the probes Ar, N₂, CO and NO. In the case of Ne, both types of oscillation are resolved in the data. Analysis of those systems for which rapid oscillations are resolved is presented on the basis of the IOS approximation, allowing the anisotropy in the potential surfaces to be probed. In the case of the other systems a simple analysis was used to estimate the effective well depths.

The anisotropies of all interactions follow the sequence C₄H₂ > C₃H₄ > C₂H₄ > C₂H₂; also, the strength of the interactions follows the same sequence, in line with changes in molecular polarisabilities. Somewhat surprisingly, the well depths of the He systems are anisotropic whereas those of the H₂ systems are isotropic. A full understanding of the potential energy surfaces will only be obtained when more experimental information, including inelastic cross sections and spectroscopic data on van der Waals clusters, is available.

Acknowledgments

The measurements described in this paper were made on an instrument designed and constructed in the Atomic and Molecular Physics Laboratories at the Australian National University during a period when Professor R. W. Crompton was its Head. ROW is especially grateful for the kindness, understanding, and general support that Bob Crompton gave to him at that stage in his career. It is a pleasure to have this paper published in the present collection from Crompton colleagues over many years.

The experimental work was done at the University of Washington with financial support from the National Science Foundation and the Pacific Northwest National Laboratory of Battelle. Analysis was undertaken in Melbourne with support from the University of Melbourne through the Rowden White Foundation.

References

- Amos, Y. T., and Yoffee, J. A. (1976). *Chem. Phys. Lett.* **39**, 53.
Armitage, J. B., Jones, E. R. H., and Whiting, M. C. (1951). *J. Chem. Soc.* **9**, 44.
Barker, J. A., and Bobetic, M. V. (1970). *Phys. Rev. B* **2**, 4169.
Barker, J. A., and Pompe, A. (1968). *Aust. J. Chem.* **21**, 1683.
Beck, R. D., Maki, A. G., Tseng, S., and Watts, R. O. (1993). *J. Mol. Spec.* **158**, 306.
Bernstein, R. B. (Ed.) (1979a). 'Atom-Molecule Collision Theory: A Guide for the Experimentalist', pp. 111-191 (Plenum: New York).
Bernstein, R. B. (Ed.) (1979b). 'Atom-Molecule Collision Theory: A Guide for the Experimentalist', pp. 301-51 (Plenum: New York).
Boughton, C. V., Miller, R. E., and Watts, R. O. (1986). *Mol. Phys.* **58**, 827.
Bryant, G. W., Eggers, D. F., and Watts, R. O. (1988). *J. Chem. Soc., Faraday Trans. 2* **84**, 1443.
Buck, U., Ettischer, I., Schlemmer, S., Yang, M., Vohralik, P., and Watts, R. O. (1993). *J. Chem. Phys.* **99**, 3494.
Buck, U., Kohl, K. H., Kohlhase, A., Faubel, M., and Staemmler, V. (1985a). *Mol. Phys.* **55**, 1255.

- Buck, U., Kohlhase, A., Phillips, T., and Secrest, D. (1983). *Chem. Phys. Lett.* **98**, 199.
- Buck, U., Kohlhase, A., Secrest, D., Phillips, T., Scoles, G., and Grein, F. (1985*b*). *Mol. Phys.* **55**, 1233.
- Buckingham, A. D., Fowler, P. W., and Hutson, J. M. (1988). *Chem. Rev.* **88**, 963.
- Danielson, L. J., Keil, M., and Dunlop, P. J. (1988). *J. Chem. Phys.* **88**, 4218.
- Danielson, L. J., Mcleod, K. M., and Keil, M. (1987). *J. Chem. Phys.* **87**, 239.
- Este, G. O., Knight, D. G., Scoles, G., Vallbusa, U., and Grein, F. (1983). *J. Phys. Chem.* **87**, 2772.
- Fluendy, M. A. D., and Lawley, K. P. (1973). 'Chemical Applications of Molecular Beam Scattering' (Chapman and Hall: London).
- Moszynski, R., Wormer, P., and van der Avoird, A. (1995). *J. Chem. Phys.* **102**, 8385.
- Nesbitt, D. J., Nibler, J. W., Schiffman, A., Chapman, W. B., and Hutson, J. M. (1993). *J. Chem. Phys.* **98**, 9513.
- Pack, R. T. (1976). *J. Chem. Phys.* **64**, 1659.
- Pack, R. T. (1978). *Chem. Phys. Lett.* **55**, 197.
- Parker, G. A., and Pack, R. T. (1978). *J. Chem. Phys.* **68**, 1585.
- Schiffman, A., Chapman, W. B., and Nesbitt, D. J. (1996). *J. Phys. Chem.* **100**, 3402.
- Scoles, G. (Ed.) (1988). 'Atomic and Molecular Beam Methods', Vol. 1, pp. 499-524 (Oxford University Press: New York).
- Weida, M. J., Sperhac, J., Nesbitt, D. J., and Hutson, J. M. (1994). *J. Chem. Phys.* **101**, 8351.
- Yang, M., and Watts, R. O. (1994*a*). *J. Chem. Phys.* **100**, 3582.
- Yang, M., and Watts, R. O. (1994*b*). *J. Chem. Phys.* **101**, 8784.